Environmental Science & Technology

pubs.acs.org/est

Article

Magnitude of Diffusion- and Transverse Dispersion-Induced Isotope Fractionation of Organic Compounds in Aqueous Systems

Fengchao Sun, Jan Peters, Martin Thullner, Olaf A. Cirpka, and Martin Elsner*

Cite This: *Environ. Sci. Technol.* 2021, 55, 4772−4782

Read Online

ACCESS | Metrics & More | Article Recommendations | Supporting Information

ABSTRACT: Determining whether aqueous diffusion and dispersion lead to significant isotope fractionation is important for interpreting the isotope ratios of organic contaminants in groundwater. We performed diffusion experiments with modified Stokes diaphragm cells and transverse-dispersion experiments in quasi-two-dimensional flow-through sediment tank systems to explore isotope fractionation for benzene, toluene, ethylbenzene, 2,6-dichlorobenzamide, and metolachlor at natural isotopic abundance. We observed very small to negligible diffusion- and transverse-dispersion-induced isotope enrichment factors (ε < −0.4 ‰), with changes in carbon and nitrogen isotope values within ±0.5‰ and ±1‰, respectively. Isotope effects of diffusion did not show a clear correlation with isotopologue mass with calculated power-law exponents β close to zero ($0.007 < \beta < 0.1$). In comparison to ions, noble gases, and labeled compounds, three aspects stand out. (i) If a mass dependence is derived from collision theory, then isotopologue masses of polyatomic molecules would be affected by isotopes of multiple elements resulting in very small expected effects. (ii) However, collisions do not necessarily lead to translational movement but can excite molecular vibrations or rotations minimizing the mass dependence. (iii) Solute−solvent interactions like H-bonds can further minimize the effect of collisions. Modeling scenarios showed that an inadequate model choice, or erroneous choice of β, can greatly overestimate the isotope fractionation by diffusion and, consequently, transverse dispersion. In contrast, available data for chlorinated solvent and gasoline contaminants at natural isotopic abundance suggest that in field scenarios, a potential additional uncertainty from aqueous diffusion or dispersion would add to current instrumental uncertainties on carbon or nitrogen isotope values (±1‰) with an additional ±1‰ at most.

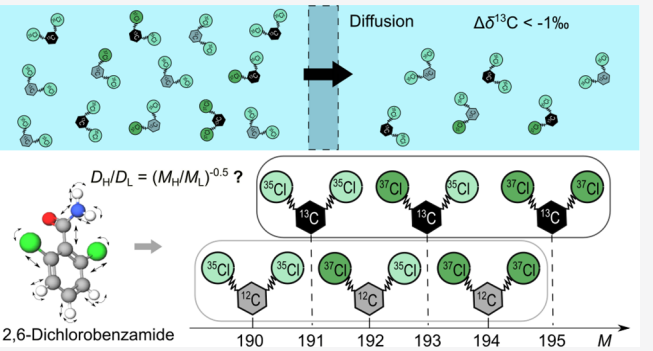

KEYWORDS: *BTEX, Compound-specific isotope analysis, Stokes diaphragm cell, Flow-through tank system, Mass dependence, Metolachlor, Organic contaminants, 2,6-dichlorobenzamide*

INTRODUCTION

Changes in compound-specific stable isotope values of organic compounds can be used to infer the extent of degradation.[1−4] In groundwater systems, solute concentrations are influenced by both (bio)chemical degradation and physical transport, namely advection, dispersion, diffusion, and interphase mass transfer.[5−8] While advection is the main mass transport process in the direction of the flow, dispersion, and diffusion cause spreading of the compounds due to the physical or chemical variability of the system. In contrast to concentrations, isotope ratios are thought to be little affected by hydrodynamic dispersion (including mechanical dispersion and diffusion) or diffusion because all isotopologues essentially undergo the same dilution.[9−12] If true, then changes in isotope values can serve as a particularly robust indicator of degradation that is little affected by these physical processes. However, it can be challenging to adequately identify and quantify the influence of dispersion and diffusion on isotope fractionation of organic compounds when evaluating the changes in isotope ratios as evidence of (bio)chemical reactions in the field. One challenge is that dispersion and diffusion may affect the concentration profiles and level out the degradation-induced gradients of the isotope ratios[5] while another complicating factor may be that the diffusion coefficients of different isotopologues differ, thus potentially causing reaction-independent isotope fractionation by the process of diffusion itself.[13]

Although such diffusion-induced isotope fractionation in the aqueous phase was repeatedly considered to be negligible,[9−12] significant diffusion-induced isotope fractionation has been reported in some studies with isotopically labeled organic compounds,[6,7,14−19] such as deuterated alcohols (with isotope

Received: October 6, 2020
Revised: February 8, 2021
Accepted: February 22, 2021
Published: March 17, 2021

enrichment factors ε between −2.6‰ and −7.0‰),[14] benzene, toluene, and ethylbenzene (ε between −40‰ and 19‰).[7,15,19] By contrast, recent studies reported negligible isotope fractionation for labeled benzene, toluene, and cyclohexane.[20,21] For compounds at natural isotopic abundance, finally, much smaller isotope fractionation has been observed, such as with CO_2,[16,22] methane,[17,18] ethane,[18] and chlorinated ethenes[6] (ε between −0.22‰ and −2.23‰).

Various theoretical models have conceptualized diffusion in the aqueous phase to be driven by intermolecular or intramolecular interactions between the solute and solvent molecules.[13,23−26] A prime focus has been on the collision of solute and solvent molecules, conceptualized as hard-sphere particles, which is usually described by the Enskog relation (eq 1),[27]

$$D_{aq} \propto \left(\frac{M_1 M_2}{M_1 + M_2}\right)^{-\beta}, \quad \beta = 0.5 \tag{1}$$

in which D_{aq}[m^2/s] is the diffusion coefficient of the solute particle in the aqueous phase, M_1 [Da] is the molecular mass of the solute, and M_2 [Da] is the molecular mass of the solvent. If in the dilute water phase the hydrogen-bonded water network is assumed to act as "effective particle",[6] then M_2 is infinitively large so that $D_{aq} \propto M_1^{-0.5}$. The resulting eq 2 is usually applied to predict the ratio of diffusion coefficients of heavy and light isotopes or isotopologues D_{aq}^H and D_{aq}^L,

$$\frac{D_{aq}^H}{D_{aq}^L} = \left(\frac{M_H}{M_L}\right)^{-\beta}, \quad \beta = 0.5 \tag{2}$$

in which M_H [Da] and M_L [Da] are the molecular masses of the heavy and light isotopes or isotopologues, respectively.

However, a power-law mass dependence of isotope fractionation with β = 0.5 has been rarely observed for aqueous-phase diffusion.[28] For noble gases, weak or negligible power-law mass-dependent isotope fractionation has been observed for Ne, Kr, and Xe with β < 0.2.[29,30] An even weaker dependence has been observed for ions (e.g., Li^+, Na^+, Cl^-, and Br^-) with β < 0.07.[13,31,32] Also for organic compounds at natural isotopic abundance, observed mass-dependent isotope fractionation was weak with β < 0.1 for trichloroethene (TCE), 1,2-dichloroethane (1,2-DCA), and *cis*-dichloroethene (*cis*-DCE).[6,7] In contrast, a much stronger mass dependence has been observed for the diffusion-induced isotope fractionation of labeled organic compounds (e.g., deuterated benzene and toluene).[7,20,21]

Mode-Coupling Theory Analysis and Molecular Dynamic Simulations were brought forward to explain the weak mass dependence of diffusion-induced isotope effects observed for noble gases and ions.[13,31,33] These theories still conceptualize the molecules of the solutes and the surrounding water as rigid masses and neglect the influence of intramolecular vibrations and rotations. The Mode-Coupling Theory assumes that diffusion can be explained by frictions in series,[13] i.e., $\frac{1}{\text{Friction}_{total}} = \frac{1}{\text{Friction}_{collisions}} + \frac{1}{\text{Friction}_{hydrodynamic}}$, in which the collision term $1/\text{Friction}_{collisions}$ would show a squared power-law mass dependence and the hydrodynamic-motion term $1/\text{Friction}_{hydrodynamic}$ shows no mass dependence at all, explaining a weaker dependence on the molecular mass, which is actually not even a power law. Considering this shaky theoretical basis, it is remarkable that all interpretations of experimental data have so far relied on the power-law mass dependence of diffusion coefficients (eq 2), merely adapting the positive exponent β. On the basis of this relationship, diffusion-induced isotope effects are hypothesized to increase in a systematic way with increasing relative mass difference between the isotopologues, where the β-value is left open for adjusting the relation between the magnitude of diffusion-induce isotope fractionation and mass difference between the isotopologues.

If there are isotope effects on molecular diffusion, then it is further still unclear how they scale up to dispersion, which describes the effective mixing and dilution in flowing groundwater. Hydrodynamic dispersion includes both mechanical dispersion caused by pore-scale velocity variations and molecular diffusion. The standard parametrization assumes that the pore diffusion coefficient D_p [m^2/s] and the mechanical dispersion $D_{mech,t/l}$ [m^2/s] are additive,

$$D_{t/l} = D_p + D_{mech,t/l} \tag{3}$$

$$D_p = \frac{1}{\tau} D_{aq} \tag{4}$$

in which the index t and l refer to the transverse and longitudinal directions, respectively, and τ [−] is the tortuosity of the porous medium. In the classical parametrization,[34] the mass dependence of molecular diffusion is relevant only at very low groundwater velocities because $D_{mech,t/l}$ is believed to be compound-independent and to scale linearly with the mean velocity v [m/s]:

$$D_{mech,t/l} = \alpha_{t/l} \cdot v \tag{5}$$

in which $\alpha_{t/l}$ is the transverse or longitudinal dispersivity [m], which is supposed to depend linearly on the effective grain diameter d_{eff} [m] in homogeneous sand packs (e.g., $\alpha_t = 3 \times d_{eff}/16$).[35]

On the basis of high-resolution transverse concentration profiles using different tracers at different velocities, however, Chiogna et al.[36] introduced a nonlinear parametrization of the transverse dispersion coefficient:

$$D_t = D_p + v \cdot \frac{d_{eff}}{\sqrt{Pe + 123}} \tag{6}$$

in which the mechanical dispersion depends on the grain-Pèclet number $Pe = v \times d_{eff}/D_{aq}$, implying that the transverse dispersion scales with the square roots of the velocity and the molecular diffusion coefficient at high velocities.

The latter work inspired many modeling studies to reconsider the isotope fractionation due to transverse dispersion in saturated porous media.[19,37−39] In such simulations, diffusion coefficients of heavy and light isotopologues were usually estimated by the Enskog[27] or the Worch relation,[40] implying an exponent β = 0.5 or 0.53 in eq 2, which resulted in large dispersion-induced isotope fractionation in these models.[15,19,37,38,41]

This study aims at experimentally re-examining isotope fractionation by diffusion and transverse dispersion for organic compounds at natural isotopic abundance. We applied compound-specific isotope analysis to investigate the diffusion-induced isotope fractionation with increasing molecular mass and decreasing mass ratio of heavy to light isotopologues for benzene, toluene, ethylbenzene, 2,6-dichlorobenzamide (BAM), and metolachlor in the aqueous phase. We determined the diffusion coefficients of the heavy and light isotopologues of each compound by conducting modified Stokes diffusion-

https://doi.org/10.1021/acs.est.0c06741
Environ. Sci. Technol. 2021, 55, 4772−4782

cell experiments.[6] We then reconsidered the mass dependence of diffusion-induced isotope fractionation by comparing the theoretical models (e.g., Enskog relation) with our measured isotope ratios and published experimental data from previous diffusion studies on labeled organic compounds, noble gases, and ions. To investigate the potential significance of isotopic effects on transverse dispersion, we conducted steady-state transport experiments in flow-through sediment tanks and compared transverse profiles with numerical-modeling results using the classical transverse dispersion parametrization and the expression of Chiogna et al., coupled to the Enskog relation.

MATERIALS AND METHODS

Diffusion Cell Experiment. The Stokes diffusion cell is a classical and commonly used approach to determine liquid-phase diffusion coefficients of dissolved species.[6,13,21,42,43] We adopted the setup of diffusion cell experiments from the design of Wanner and Hunkeler.[6] The diffusion cell was separated into upper and lower compartments (with a volume of each compartment of 38 mL) by a silica frit in between. The lower compartment was filled with a solution of the dissolved organic compound, while the upper compartment was filled with deionized water, which was continuously replaced at a pumping rate of 10 mL/min to keep the concentration in the upper compartment close to zero (Figure 1). Therefore,

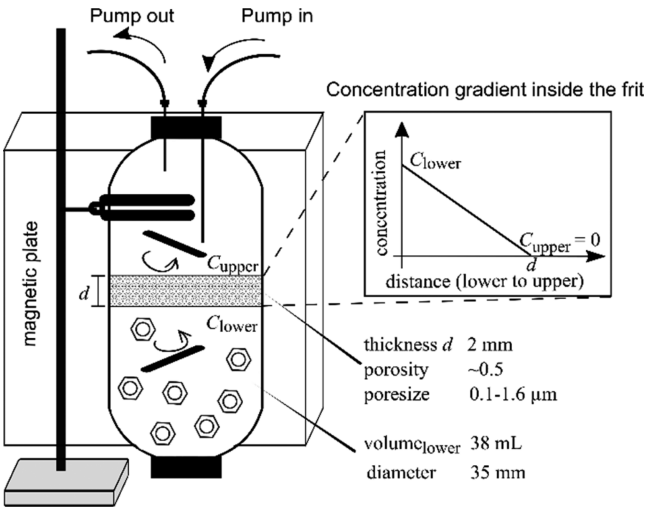

Figure 1. Setup of Stokes' diffusion cell experiment.

the isotope fractionation in the lower compartment follows a Rayleigh type behavior. The solution of each compartment was well mixed by a Teflon-coated stirring bar to ensure a homogeneous concentration distribution. Because of the concentration gradient through the frit, the small pore size, and the uniform composition in each compartment maintained by vigorous stirring, diffusion is the exclusive transport process of the dissolved organic compounds through the frit.[13,42] The design parameters and the estimation of the characteristic factor of each diffusion cell can be found in Figure 1 and Table S2 of the Supporting Information (SI). We conducted two sets of experiments: one set with benzene, toluene, and ethylbenzene; and the other with BAM and metolachlor. Experiments were performed in parallel for different durations; in each experiment the concentrations and isotope values of the solution in the lower compartment were measured at the beginning and the end of each time period.

Upon diffusion from the lower to the upper compartment through the silica frit, the concentrations in the lower compartment meet the following expression:[6]

$$C(t) = C(0)\cdot e^{-D_{aq}\cdot\sigma\cdot t} \tag{7}$$

in which $C(0)$ [mg/L] is the initial concentration in the lower compartment of the diffusion cell, and $C(t)$ [mg/L] is the concentration at time t [s]. $\sigma = \frac{\phi\cdot\tau\cdot A}{d\cdot V_{low}}$ [m^{-2}] is the cell calibration factor, with ϕ [−], τ [−], A [m^2], d [m], and V_{low}[m^3] being the porosity, tortuosity, cross-sectional area, thickness of the frit, and the volume of the lower compartment, respectively. From this we can derive a Rayleigh-fractionation equation:[6]

$$\ln\left(\frac{R_t}{R_0}\right) = \ln\left(\frac{\delta_t + 1}{\delta_0 + 1}\right) = \underbrace{\left(\frac{D_{aq}^{H}}{D_{aq}^{L}} - 1\right)}_{=\varepsilon_D} \times \ln\left(\frac{C(t)}{C(0)}\right) \tag{8}$$

in which R_0 [−] and R_t [−] represent the isotope ratios at times zero and t, respectively, δ_0 [−] and δ_t[−] are the corresponding δ isotope values [−], and $\varepsilon_D = \frac{D_{aq}^{H}}{D_{aq}^{L}} - 1$ [−] is the isotope-enrichment factor due to diffusion.

Flow-Through Sediment-Tank Experiment. To investigate the effect of transverse dispersion on the isotope fractionation of organic compounds in saturated porous media, we conducted two-dimensional flow-through sediment-tank experiments. The setup of the tank (Figure S1) was adapted from Bauer et al.[44] and is detailed in the SI. At the inlet and outlet boundaries of the tank, 16 equally spaced ports (distance 1.0 cm) were pumped with a constant rate of 45 ± 2 μL/min per port. A solution with the target compounds (inlet solution with BAM 400 mg/L and metolachlor 100 mg/L in the first setup, and inlet solution with toluene 34.2 mg/L in the second setup) at natural isotopic abundance was injected into the central inlet port (z = 8 cm) of the tank, whereas a compound-free solution was injected into the remaining inlet ports. We sampled the 16 outlet ports to obtain concentration and isotope profiles at the outflow boundary of the domain. Sampling for isotope measurements of BAM and metolachlor was conducted from day 5 to day 20; sampling for isotope measurements of toluene was conducted from day 5 to day 8.

Chemicals. A list of chemicals is provided in the SI.

Carbon and Nitrogen Isotope Analysis of BAM, Metolachlor, Benzene, Toluene, and Ethylbenzene. Samples from the tank experiments were frozen at −20 °C immediately after sampling until enough samples were collected for isotope analysis. For carbon and nitrogen isotope measurements of BAM and metolachlor, the samples from the diffusion cell experiments (40 mL) and tank experiments (1 L) were first filtered through a 0.2 μm Nalgene Rapid-Flow filter (Thermo Fisher Scientific, Germany) and concentrated in ethyl acetate after solid-phase extraction as detailed in the SI. All isotope measurements were conducted on a GC−IRMS system in which a TRACE GC Ultra gas chromatograph (Thermo Fisher Scientific, Italy) with a DB-5 analytical column (60 m, 0.25 mm i.d., 1 μm film, Agilent Technologies, Germany) was coupled to a Finnigan MAT 253 isotope-ratio mass spectrometer through a Finnigan GC Combustion III interface (Thermo Fisher Scientific, Germany). For carbon-

https://doi.org/10.1021/acs.est.0c06741
Environ. Sci. Technol. 2021, 55, 4772−4782

Table 1. Experimental Results for Measured Diffusion Coefficients D_{aq}, Diffusion Coefficient Ratios D^{H}_{aq}/D^{L}_{aq} of Heavy to Light Isotopologues, Isotope Enrichment Factors ε and Calculated β-Values of Organic Compounds at Natural Isotope Abundance from This Study and Literature[a]

compound	isotopologues	D^{H}_{aq}/D^{L}_{aq}	ε (‰)	β	D_{aq}-measured (m^2/s)	references
CO_2	$^{13}CO_2$/ CO_2[b]	0.99927 ± 0.00019	−0.73 ± 0.19	0.032 ± 0.009		O'Leary, 1984[16]
	$^{13}CO_2$/ CO_2[c]	0.99913 ± 0.00005	−0.87 ± 0.05	0.039 ± 0.002		Jahne et al.,1987[22]
CH_4	$^{13}CH_4$/ CH_4[b]	0.9978 ± 0.0008	−2.23 ± 0.82	0.037 ± 0.014		Zhang and Krooss, 2001[17]
	$^{13}CH_4$/ CH_4[b]	0.9978 ± 0.0012	−2.17 ± 1.12	0.036 ± 0.023		Schloemer and Krooss, 2004[18]
C_2H_6	$^{13}CCH_6/C_2H_6$[b]	0.9988 ± 0.0008	−1.23 ± 0.76	0.038 ± 0.023		Schloemer and Krooss, 2004[18]
DCM	$^{13}CH_2Cl_2$/ CH_2Cl_2[b]	0.99972 ± 0.0009	−0.28 ± 0.09	−0.025 ± 0.008		Wanner et al., 2017[45]
cis-DCE	$C_2H_2{}^{37}ClCl/C_2H_2Cl_2$[b,d]	0.9982 ± 0.0003	−1.80 ± 0.3	0.088 ± 0.017		Jin et al., 2014[7]
1,2-DCA	$^{13}CCH_4Cl_2$/ $C_2H_4Cl_2$	0.99977 ± 0.00004	−0.23 ± 0.04	0.023 ± 0.004		Wanner and Hunkeler, 2015[6]
	$C_2H_4{}^{37}ClCl/C_2H_4Cl_2$	0.99939 ± 0.00003	−0.61 ± 0.03	0.031 ± 0.002		Wanner and Hunkeler, 2015[6]
TCE	$^{13}CCHCl_3$/ C_2HCl_3	0.99978 ± 0.00006	−0.22 ± 0.06	0.029 ± 0.008		Wanner and Hunkeler, 2015[6]
	$C_2H^{37}Cl_2$/ C_2HCl_3	0.99963 ± 0.00003	−0.37 ± 0.03	0.024 ± 0.002		Wanner and Hunkeler, 2015[6]
	$C_2H^{37}Cl_2$/ C_2HCl_3[b,d]	0.9993 ± 0.0002	−0.67 ± 0.2	0.043 ± 0.009		Jin et al., 2014[7]
Benzene	$^{13}CC_5H_6/C_6H_6$	0.99991 ± 0.00001	−0.09 ± 0.01	0.007 ± 0.001	(11.2 ± 3.2) × 10^{-10}	this study
Toluene	$^{13}CC_6H_8/C_7H_8$	0.99991 ± 0.00006	−0.09 ± 0.06	0.008 ± 0.006	(10.6 ± 4.2) × 10^{-10}	this study
Ethylbenzene	$^{13}CC_7H_{10}/C_8H_{10}$	0.99991 ± 0.00005	−0.09 ± 0.05	0.010 ± 0.005	(10.4 ± 4.8) × 10^{-10}	this study
BAM	$^{13}CC_6H_5Cl_2NO/C_7H_5Cl_2NO$	0.99992 ± 0.00016	−0.08 ± 0.16	0.015 ± 0.030	(6.08 ± 0.51) × 10^{-10}	this study
	$C_7H_5Cl_2{}^{15}NO/C_7H_5Cl_2NO$	0.99980 ± 0.00022	−0.20 ± 0.22	0.038 ± 0.042		
Metolachlor	$^{13}CC_{14}H_{22}ClNO_2/C_{15}H_{22}ClNO_2$	0.99964 ± 0.00036	−0.36 ± 0.36	0.102 ± 0.102	(5.02 ± 0.56) × 10^{-10}	this study
	$C_{15}H_{22}Cl^{15}NO_2$/ $C_{15}H_{22}ClNO_2$	0.99994 ± 0.00035	−0.06 ± 0.35	0.017 ± 0.099		

[a]Uncertainties of D_{aq}-values were the standard deviation, uncertainties of D^{H}_{aq}/D^{L}_{aq}- and ε-values were calculated based on the 95% confidence intervals of regressions according to eq 8. Also, literature data were evaluated with respect to 95% confidence intervals to enable comparisons on an equal basis. Uncertainties of β-values were calculated based on Gauss' error propagation law by using the uncertainty of D^{H}_{aq}/D^{L}_{aq}. [b]Uncertainties of D^{H}_{aq}/D^{L}_{aq}- and ε-values represent the recalculated 95% confidence interval based on the published standard deviation or data set; uncertainties of β-values were calculated based on Gauss' error propagation by using the uncertainty of D^{H}_{aq}/D^{L}_{aq}. [c]Uncertainties of D^{H}_{aq}/D^{L}_{aq}- and ε-values were published system deviations; uncertainties of β-values were calculated based on Gauss' error propagation by using the uncertainty of D^{H}_{aq}/D^{L}_{aq}. [d]D^{H}_{aq}/D^{L}_{aq}-, ε-, and β-values were calculated based on D^{96}_{cisDCE}, D^{98}_{cisDCE}, D^{130}_{TCE}, and D^{132}_{TCE} values in Table S2 from Jin et al.[7]

https://doi.org/10.1021/acs.est.0c06741
Environ. Sci. Technol. 2021, 55, 4772−4782

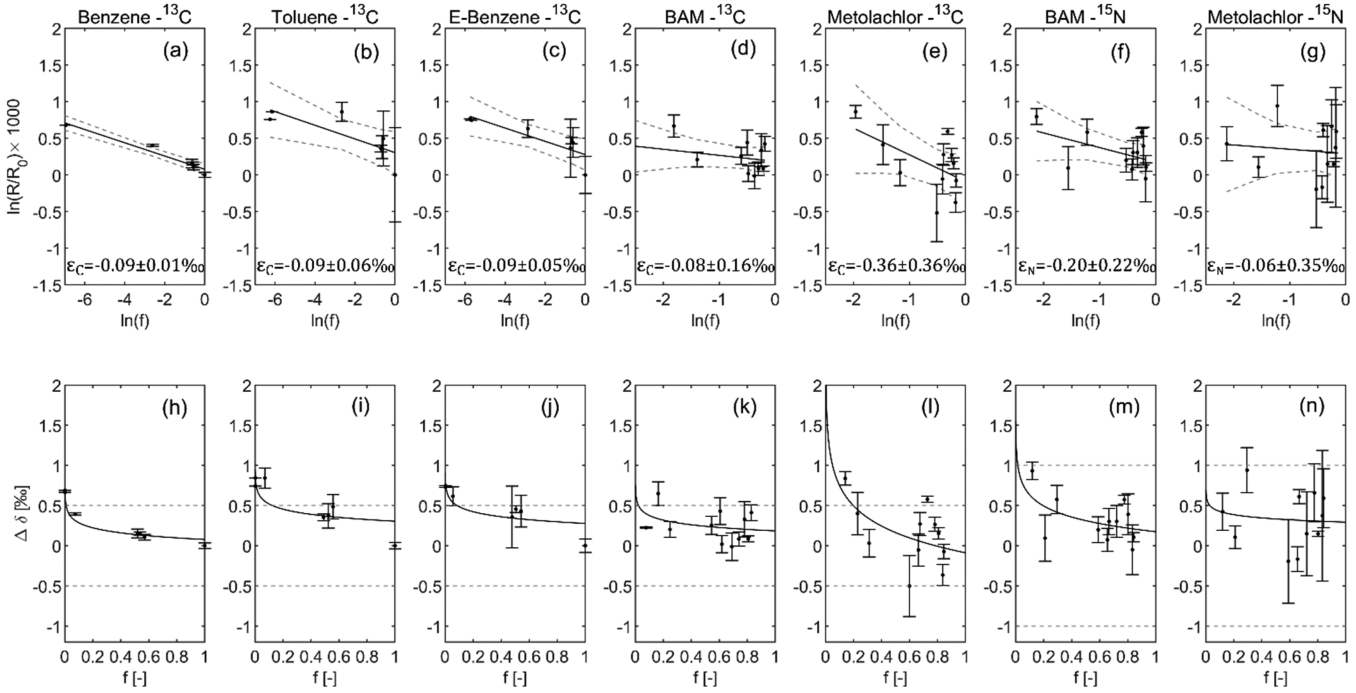

Figure 2. Diffusion-induced isotope fractionations observed for benzene, toluene, ethylbenzene, BAM, and metolachlor. Panels (a−g) represent evaluations of the isotope fractionation factor ε of each compound according to the Rayleigh equation (eq 8) with 95% confidence intervals. Dashed lines indicate 95% confidence intervals of the regression line. Panels (h−n) represent the correlation between the remaining concentration fractionation $f(C(t)/C(0))$ and $\Delta\delta^{13}C$ for each compound and $\Delta\delta^{15}N$ for BAM and metolachlor. Dashed lines indicate the instrument uncertainties of ±0.5‰ for carbon-isotope measurements and of ±1‰ for nitrogen-isotope measurements. Error bars represent standard deviations of the measurements.

isotope measurements of benzene, toluene, and ethylbenzene, a Velocity XPT purge-and-trap sample concentrator with an AQUATek 70 liquid autosampler (Teledyne Tekmar, Mason, OH) was connected to the gas chromatograph. Detailed information about the method can be found in the SI.

Concentration Measurements. BAM and metolachlor concentrations were measured using a Prominence HPLC system (Schimadzu Corp., Japan) with a 75 × 4.6 mm^2 Kinetex 2.6 μm C18 100 Å column (Phenomenex Inc., Golden, CO). Benzene, toluene, and ethylbenzene concentrations were measured on a Trace DSQ GC-MS system (Thermo Electron, Germany) equipped with a Combi PAL autosampler (CTC Analytics, Switzerland) with a DB-5 analytical column (30 m, 0.25 mm i.d., 0.5 μm film, Agilent Technologies, Germany). Chloride (Cl^-) concentrations in the diffusion-cell experiments were analyzed by ion chromatography (Dionex 500, Dionex, Sunnyvale, CA). Concentrations of the conservative tracer uranine in the tank experiment were measured on VICTOR Multilabel Plate Reader (PerkinElmer, U.S.A.). A detailed description of the methods is provided in the SI.

Governing Equations and Numerical Method. The solute transport in the 2D flow-through sediment-tank was described by the following advection-dispersion partial differential equation in two dimensions:

$$\frac{\partial C_i}{\partial t} = -\mathbf{v}\cdot\nabla C_i + \nabla\cdot(\mathbf{D}\cdot\nabla C_i) \quad (9)$$

in which C_i [μmol L^{-1}] are the concentrations of BAM with heavy (e.g., ^{13}C or ^{15}N) or light isotopes (e.g., ^{12}C or ^{14}N), respectively; $\mathbf{D}$ [m^2 s^{-1}] is the dispersion tensor; $\mathbf{v}$ [m s^{-1}] is the velocity vector; and t[s^{-1}] is time.

We compared the transverse dispersion behavior of heavy and light isotopologues in the modeling scenarios with the classical transverse dispersion equation (eq 5) and the Chiogna et al. transverse dispersion equation (eq 6) in MATLAB. The solute transport process was solved in the homogeneous domain with a spatial discretization of 1 mm in vertical direction and 10 mm in horizontal direction by the Finite Volume Method. Global implicit method was adopted for the transport.

RESULTS AND DISCUSSION

Diffusion Cell Experiments Showed Weak to Negligible Diffusion-Induced Isotope Fractionation of Organic Compounds at Natural Isotopic Abundance. The initial and final concentrations of benzene, toluene, ethylbenzene, BAM, and metolachlor in the lower compartment of the diffusion cell in each of the experiments conducted over different time periods can be found in Table S1. Concentrations of all organic compounds in the lower compartments of the diffusion cells decreased with extending experimental duration and followed eq 7 (Figure S2). Table 1 shows the diffusion coefficients of the compounds calculated according to eq 7, which are in the upper range of the literature values (Table S3) within uncertainties.

Even after an extended duration of diffusion, and with target compounds at low remaining concentrations (down to 0.1% of initial values) carbon- and nitrogen-isotope values $\Delta\delta$ of all investigated organic compounds fell within a range of −1‰, which essentially coincides with the uncertainty of ±0.5‰ for carbon-isotope measurements and of ±1‰ for nitrogen-isotope measurements, respectively (Figure 2). When isotope enrichment factors ε_C for carbon and ε_N for nitrogen were

https://doi.org/10.1021/acs.est.0c06741
Environ. Sci. Technol. 2021, 55, 4772−4782

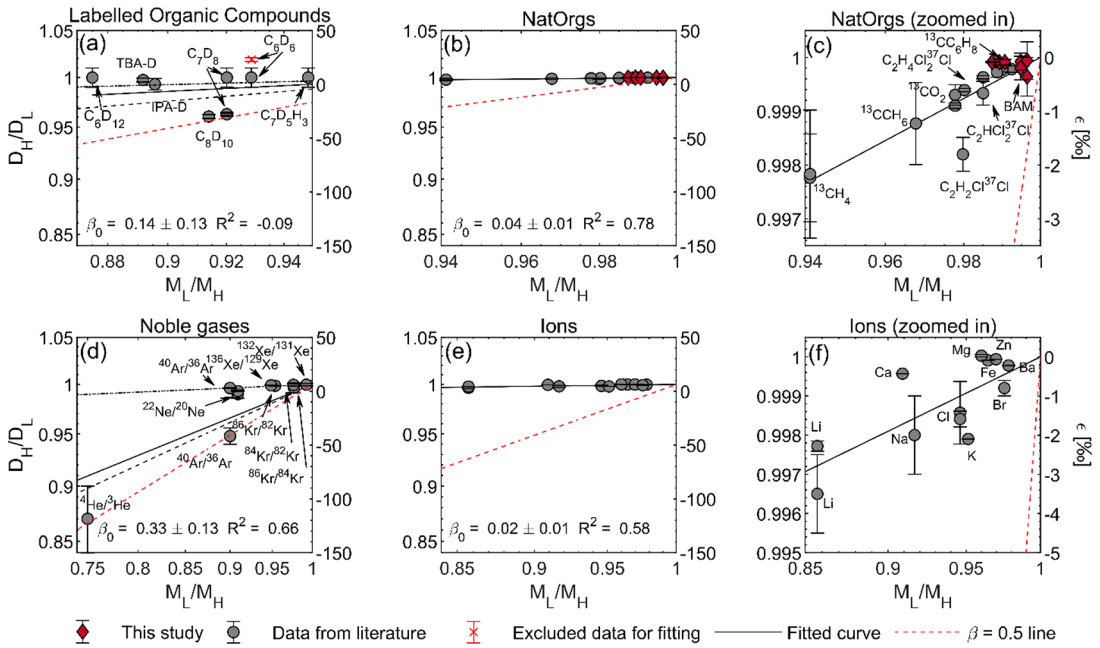

Figure 3. D_H/D_L (left y axis) as a function of M_L/M_H in logarithmic scale, corresponding to the enrichment factor ε [‰] on the right y axis. For organic compounds at natural isotopic abundance (NatOrgs), M_L/M_H was calculated based on the most abundant isotopologues with one or zero heavy isotopes in one molecule. Solid lines show the determination of β_0 by a regression curve based on eq 2, where red crosses represent data excluded from the fit. Red dashed lines represent calculated trends in isotope values with $\beta = 0.5$. In panel (a), the black dashed line represents the regression ($\beta_0 = 0.24$) without the data of labeled benzene, toluene and cyclohexane with $D_H/D_L = 1$,[20,21] and the black dashed-dotted line represents the regression ($\beta_0 = 0.07$) without the data of labeled toluene and ethylbenzene with comparatively small D_H/D_L-values.[15] In panel (d), the black dashed line represents the regression ($\beta_0 = 0.37$) without the anomalously high D_H/D_L value of Ar isotopes,[46] and the black dash-dotted line represents the regression ($\beta_0 = 0.04$) without low D_H/D_L-values of Ar and He isotopes data.[22,30] Most of the compounds data points are labeled with compound names except for some of the NatOrgs due to the limit of space. Error bars represent the uncertainties listed in Tables 1 and S5. Detailed data are available in Tables 1 and S5.

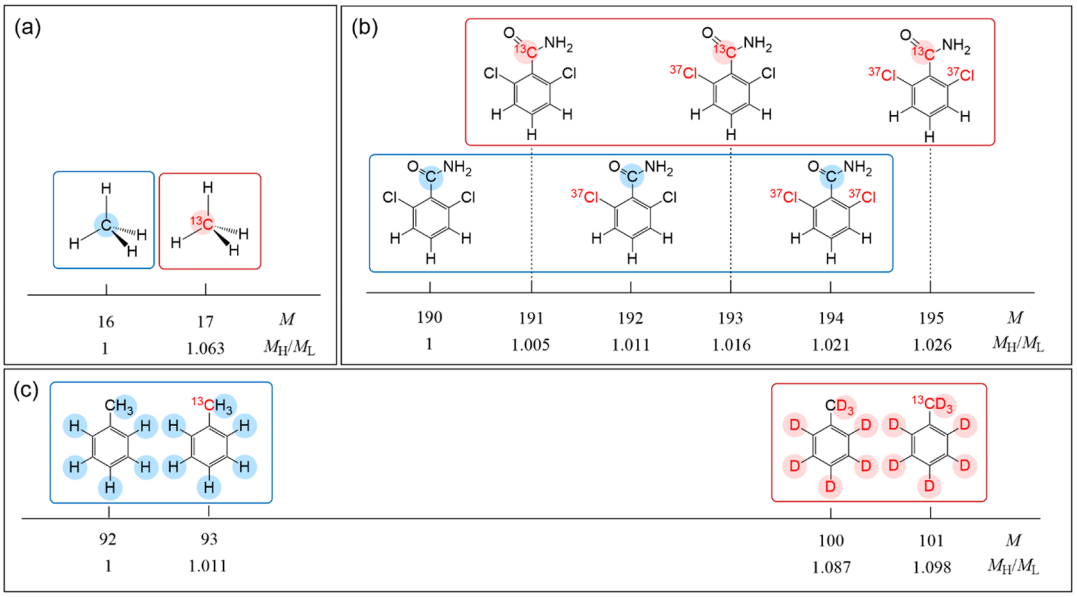

Figure 4. Mass and mass ratio of heavy to light isotopologues of (a) methane and (b) BAM at natural isotopic abundance, and (c) deuterated and nondeuterated toluene.

calculated based on the Rayleigh equation (eq 8), values were smaller than −0.36‰ corresponding to a diffusion coefficient ratio for each organic compound isotopologue pair of close to 1.0 (Table 1). Therefore, the observed isotope fractionation induced by diffusion of benzene, toluene, ethylbenzene, BAM, and metolachlor at natural isotopic abundance in aqueous phase was weak to negligible.

The calculated β-values of the isotopologue pairs for our target compounds are without exception smaller than 0.1 showing a similarly weak mass dependence as observed in other studies[6,7,16−18] for CO_2, CH_4, C_2H_6, TCE, 1,2-DCA, and

https://doi.org/10.1021/acs.est.0c06741
Environ. Sci. Technol. 2021, 55, 4772−4782

cis-DCE at natural isotopic abundance (Table 1). This dependence is particularly weak when compared to much larger β-values (β = 0.4 to 0.5) reported for labeled toluene and ethylbenzene[7,15,19] (Figure 3; note that we have omitted stark outliers from labeled studies in this comparison, which will be discussed later on). This raises the question of the underlying reasons for the different behavior of labeled and nonlabeled organic compounds.

If a mass dependence is hypothesized based on collision theory, then diffusion-induced isotope fractionation depends on differences in molecular mass, irrespective of the element of the isotopic substitution by which these mass differences are caused (eq 2). In order to illustrate two important influences, Figure 4 shows molecular masses of isotopologues and the mass ratios of heavy to light isotopologues of labeled and nonlabeled organic compounds. The first, widely recognized, influence is that compounds at natural isotopic abundance show a much smaller relative mass difference than labeled substances so that also the expected fractionation is much smaller. This consequence is exemplified in the mass ratios of M_H/M_L = 93/92 = 1.01 for ^{13}C-substituted toluene vs M_H/M_L = 100/92 = 1.09 for perdeuterated toluene in Figure 4c, and it is the underlying reason for the hypothesized power law dependence of eq 2. The second, possibly less obvious influence is illustrated by comparing the mass and mass ratio of heavy to light isotopologues of methane, BAM, and perdeuterated toluene in Figure 4. Perdeuterated isotopologues are clearly separated in mass from nonlabeled toluene isotopologues, and this separation is not significantly affected by the additional isotopic substitution of ^{13}C at natural abundance (Figure 4c). In the case of methane (Figure 4a) isotopologues of mass 17 at natural isotopic abundance can be derived from substitution by either ^{13}C or ^{2}H. Due to the low natural abundance of ^{2}H, however, isotopologues of mass 17 are almost exclusively composed of $^{13}CH_4$ so that also here, mass separation can be attributed to only one specific element (^{13}C vs ^{12}C, Figure 4a). Figure 4b illustrates that this is different with isotopes of different elements in a multielement organic compound at natural isotopic abundance such as BAM. Here, substitution by isotopes of other elements (e.g., ^{37}Cl, ^{15}N) lends isotopologues a higher molecular mass, even though they may contain only ^{12}C. Hence, isotope separation of ^{13}C vs ^{12}C within the isotopologues can never be as sharp as that for methane or labeled organic compounds. While this effect may be taken into account by explicitly modeling all isotopologues including all elements,[7] it is neglected by a power-law mass dependence that concentrates on only one element. However, Figure 3c suggests that such an approach may not even be adequate. The diffusion isotope effects of BAM, toluene, and methane do not follow the same trend, where toluene shows much smaller isotope effects than expected from the regression line between methane and BAM. This warrants a closer critical evaluation of this widely postulated mass dependence.

Critical Evaluation of the Mass Dependence of Diffusion-Induced Isotope Fractionation. To further investigate the relation between diffusion-induced isotope fractionation and the mass ratio of heavy-to-light isotopes or isotopologues, we compared the mass dependence of organic compounds at natural isotopic abundance, labeled organic compounds, ions, and noble gases (Figure 3) by estimating β_0 based on eq 2. To qualitatively understand the factors affecting diffusion-induced isotope fractionation of organic compounds, we first considered noble gases and ions as monatomic species with either very strong (ions), or very weak (noble gases) solute−solvent interactions.

Diffusion of ions in water shows small isotope fractionation (M_L/M_H > 0.95, $|\varepsilon|$ < 2‰), with a very weak to negligible mass dependence of diffusion coeffficients of β_0 = 0.02 ± 0.01. Strong ionic interactions between water molecules and charged ions lead to an intimately bound solvation shell around the ions.[31] Hence, collisions between ions and surrounding water molecules are not expected to directly lead to translational movement of the ion, but rather to vibrations and rotations within the network of hydrogen bonds inside the solvation shell.[31] In contrast, for noble gases the mass dependence of diffusion-induced isotope fractionation in the aqueous phase is inconsistent, with β_0 = 0.33 ± 0.13 when all data are included. For indiviual isotope pairs of Ne, Kr, and Xe, the determined β-values vary between −0.09 and 0.192,[29,30,46,47] whereas Ar showed an inconsistent mass dependence with β = 0.508 in the study of Tyroller et al.[30] and β = 0.035 and 0.037 in the study of Tempest and Emerson[46] and Seltzer et al.[47] Similar to the strong mass dependence of Ar observed by Tyroller et al.,[30] the β-value of He reported by Jähne et al.[22] is also high (β = 0.486). Since noble gases are monatomic gases without the formation of ionic or hydrogen bounds with water, the picture of collisions between simplified hard spheres (i.e., solute and solvent molecules) in the Enskog relation seems to be appropriate at first sight. However, the weak mass dependence of Ne, Kr, and Xe isotope fractionation and the contradictory mass dependence of Ar put this picture into question. Molecular-dynamic simulations have suggested that the coupling of short-range and long-range interactions may lead to the weak mass dependence of Ne, Kr, and Xe; while quantum tunneling might be the reason for the strong mass dependence of He[13,31,33] and the mass dependence of Ar diffusion-induced isotope fractionation is still under debate.

Among the labeled organic compounds (Figure 3a), deuterated isopropyl alcohol (IPA) and *tert*-butyl alcohol (TBA) showed comparatively low diffusion-induced isotope effects. In contrast to benzene, toluene, or ethylbenzene (Figure 3a), these alcohols can form hydrogen bonds resulting in strong interactions with water molecules. In a similar way as with ionic interactions of dissolved ions (Figure 3f), such strongly directed interactions in the solvent shell may compete with the short-range interaction following the Enskog relation so that they weaken the mass dependence of diffusion. In this light the data in Figure 3a suggest that a power-law dependence on molecular mass may not necessarily be observable across all organic molecules. Instead, the compound-specific ability to undergo specific interactions with solvent molecules (dependent on functional groups) may be an important factor unaccounted for in the Enskog relation. Another compound-specific factor that is not considered are molecular vibrations and rotations. In collision theory, organic molecules are treated as single solid balls, even though they consist of multiple atoms and bonds. Each molecule has its degree of freedom which is the sum of translation, rotation, and vibration modes. Treating a polyatomic molecule such as toluene like a noble gas is therefore a gross simplification, even though it may have a similar molecular mass (e.g., Kr: 84, toluene: 92). While for Kr every collision leads to a (short-range) translational movement, collisions of toluene may excite rotations and vibrations instead, which do not result in molecular diffusion. Hence, omitting vibrations and rotations is

https://doi.org/10.1021/acs.est.0c06741
Environ. Sci. Technol. 2021, 55, 4772−4782

likely a further confounding factor to the simplified description by eq 2.

Finally, stark outliers have been reported for labeled molecules, where the inconsistent diffusion-induced isotope fractionation of labeled benzene and toluene in different experimental setups stand out. Rolle et al.[15] observed significant normal diffusion-induced isotope fractionation for labeled toluene and ethylbenzene, and reverse isotope fractionation for labeled benzene, whereas Kopinke et al.[20] reported negligible isotope fractionation of labeled benzene, toluene, and cyclohexane and hypothesized that the different solvent matrix (aqueous diffusion in agar gel vs water) may induce the contradictory mass dependence. Presently, it is difficult to explain this inconsistency—future studies may explore whether it can be traced back to specific features of the experimental setups, or even to measurement protocols, the linearity and accuracy of which are not as stringently established for GC−MS as for GC−IRMS. Currently it can therefore be concluded that perdeuterated compounds appear to be poor models for studies of aqueous diffusion of organic compounds at natural isotopic abundance.

For organic compounds at natural isotopic abundance (Figure 3b, c), in contrast, a comparatively consistent picture emerges: β-values are generally smaller than 0.1 and the fitted β_0 of 0.04 indicates a weak to negligible mass dependence. Specifically, the enrichment factor of the diffusion-induced isotope fractionation $|\varepsilon|$ is smaller than 1‰ when $M_L/M_H > 0.98$. Only CO_2, methane, and ethane are reported to exhibit higher enrichment factors due to the large mass difference between heavy and light isotopologues, and the negligible interference by isotopes of other elements (disscussed in Figure 4). In summary, our critical discussion of the mass-dependence of isotope fractionation provides multiple arguments as to why a power law with $\beta = 0.5$ as expressed in the Enskog relation is not adequate for organic compounds at natural isotopic abundance. First, as discussed in the Introduction, this relationship is inconsistent with the Mode-Coupling Theory. Second, solute−solvent interactions and, third, intramolecular movements are neglected. Fourth, the equation applies to multiatomic isotopologues rather than isotopes. Threrefore, data from compound-specific isotope analysis by GC−IRMS cannot be directly evaluated. Finally, our considerations show that data on labeled compounds cannot be extrapolated to model substances at natural isotopic abundance. In particular, an exponent of $\beta = 0.5$ is not adequate and would lead to a gross overestimation of diffusion-induced isotope effects. In contrast, our data obtained with BTEX contaminants and pesticides, which all contained at least 6 carbon atoms per molecule, gave very small $^{13}C/^{12}C$ and $^{15}N/^{14}N$ isotope effects of aqueous diffusion: between −0.1‰ and −0.4‰. This magnitude is in agreement with $^{13}C/^{12}C$ effects between −0.2‰ and −0.3‰ determined by Wanner and Hunkeler[6] in the same Stokes' cell setup for diffusion of representative chlorinated groundwater pollutants (trichloroethylene, dichloroethane, and dichloromethane).[6,45] In combination, these data put an upper limit of about −0.2‰ to −0.4‰ to the magnitude of aqueous diffusion isotope effects to be expected for typical pollutants at contaminated sites including petroleum and chlorinated hydrocarbons (but not natural gas constituents such as methane, ethane, etc.). Under these boundary conditions, simulations of Wanner and Hunkeler for low permeability sediments (aquitards) suggest that the resulting diffusion-induced changes in $\delta^{13}C$-values would be below $\Delta\delta^{13}C = 1.5‰$.[6]

Two-Dimensional Flow-through Sediment Tank Experiments Showed Negligible Isotope Fractionation by Transverse Dispersion. Figure 5 shows the steady-state,

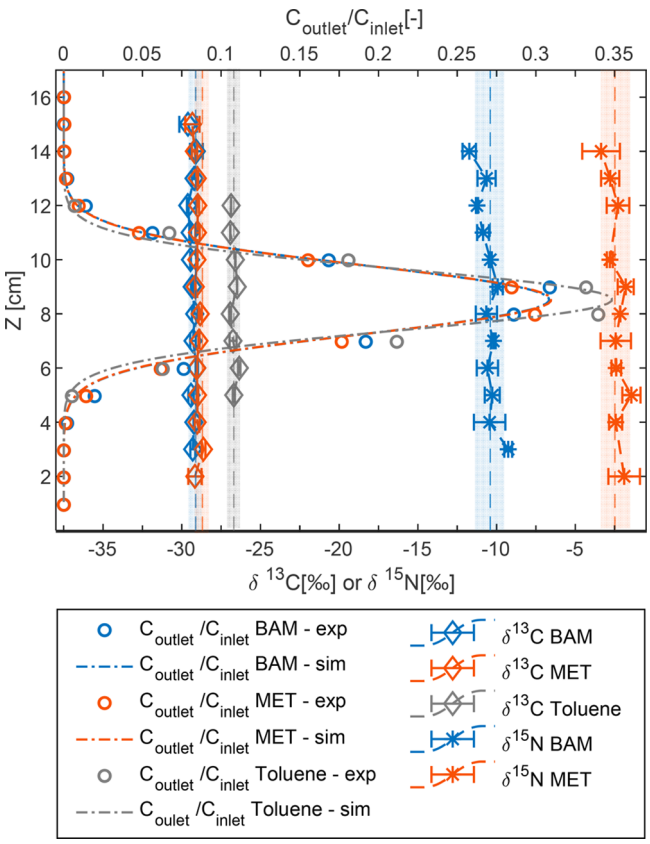

Figure 5. Measured concentrations, $\delta^{13}C$- and $\delta^{15}N$-values of BAM and MET, and $\delta^{13}C$-values of toluene at the outlets of the tank. Dash-dotted lines indicate fitted numerical simulations for conservative transport. Error bars represent standard deviations of the measurements. Color zones with dashed lines represent ±0.5‰ uncertainty for the standard C isotope values and ±1‰ uncertainty for the standard N isotope values.

conservative, transverse profiles of concentrations and isotope values of BAM, metolachlor, and toluene in the outflow of the flow-through tank. The transverse concentration profiles meet the expected Gaussian distributions. The fitted transverse dispersion coefficients of BAM, metolachlor, and toluene were 2.99×10^{-9} m^2/s, 2.94×10^{-9} m^2/s, and 1.72×10^{-9} m^2/s, respectively. Additional modeling parameters can be found in Table S4.

As shown in Figure 5, the $\delta^{13}C$- and $\delta^{15}N$-values of BAM were in the range of −29.6‰ to −29.0‰ and −11.7‰ to −9.3‰, respectively, the $\delta^{13}C$ and $\delta^{15}N$ values of metolachlor were in the range of −29.3‰ to −28.6‰ and −3.4‰ to −1.4‰, respectively, whereas the $\delta^{13}C$-values of toluene were in the range of −26.9‰ to −26.3‰. In general, the absolute difference between the observed isotope values and the standard isotope values of the target compounds was smaller than 0.5‰ for carbon, and smaller than 1‰ for nitrogen. Thus, we did not observe significant isotope fractionation induced by transverse dispersion that was above the uncertainty of the analytical methods (±0.5 for carbon or

https://doi.org/10.1021/acs.est.0c06741
Environ. Sci. Technol. 2021, 55, 4772−4782

±1‰ for nitrogen, respectively), even at very small concentrations (C_{outlet}/C_{inlet} < 0.1‰) at the top and bottom of the tank. This observation is consistent with previous observations of negligible BAM isotope fractionation by transverse dispersion in a mesoscale aquifer model.[48]

■ ENVIRONMENTAL SIGNIFICANCE

The parametrization of Chiogna et al. leads to a square-root dependence of the transverse dispersion coefficient on the diffusion coefficient at high velocities, which predicts significant isotope fractionation by transverse dispersion if the diffusion coefficient is assumed to be strongly mass dependent. Numerous published solute-transport models[15,19,37,38,41] coupled the parametrization of Chiogna et al. to the Enskog or Worch equations to compute the isotopologue-specific transverse dispersion coefficients of organic contaminants. In combination with the use of labeled substrates, β-values as high as 0.5 (e.g., β = 0.53 for PCE,[41] ethylbenzene,[38] and deuterated ethylbenzene[19]) were assumed. For a critical re-evaluation in the light of this study's evidence, we simulated the expected isotope fractionation in advective-dispersive transport of heavy and light isotopologues of BAM. They were treated as distinct species with different diffusion coefficients following eq 2 in the 2D flow-through system in two scenarios using (a) the classical linear equation (eq 5), and (b) the Chiogna et al. equation (eq 6) to parametrize the transverse dispersion. We used β-values of 0.01, 0.1, and 0.5 and showed the computed dispersion-induced isotope fractionation in Figure 6. Both scenarios showed negligible isotope fractionation (|Δδ| < 1‰) when the mass dependence of the diffusion was weak (β = 0.01). As expected, the computed isotope fractionation induced by transverse dispersion was larger and more sensitive to β-values in scenario (b) with the Chiogna et al. parametrization than in scenario (a).

In addition, we simulated isotope fractionations $\Delta\delta_{max}$ at the outmost vertical outlet port of the tank system induced by transverse dispersion as a function of β and the mass ratio of heavy-to-light isotopologues M_H/M_L (Figure S3). Consistent with the simulations in Figure 6, the Δδ-values predicted by the parametrization of Chiogna et al. (Figure S3a,c) are about twice as large as those predicted by the classical equation (Figure S3b,d). The results also indicate that both scenarios predict very large isotope fractionations when a β-value of 0.5 is assumed; for M_H/M_L = 1.05, Δδ = −25.4‰ using the classical parametrization, and with Δδ = −66.7‰ using the Chiogna et al. parametrization. As such strong isotope fractionation has not been observed, these results strengthen the point that the Enskog and Worch relations with β = 0.5 or 0.53 greatly overestimate the isotope fractionation induced by diffusion and transverse dispersion.

In contrast, our diffusion experiments, the other studies presented in Figure 3, and the results from our tank experiments suggest that the mass dependence of diffusion coefficients is weak or negligible, especially for organic compounds at natural isotopic abundance. Available data (Table 1) suggest that organic compounds at natural isotopic abundance show small to negligible diffusion- and dispersion-induced isotope effects with isotope enrichment factors ε < −0.4‰. With ε < −0.4 ‰, the simulated Δδ in our tank system (with $D_t = 2.99 \times 10^{-9}$ m²/s) is smaller than −1.2‰ even using eq 6 from Chiogna et al. (Figure 6, red zone). For the simulation at even lower remaining concentrations (C_{outlet}/C_{inlet} = 10^{-11}; Figure S4, simulation with $D_t = 1.5 \times 10^{-9}$ m²/s) the estimated Δδ (with ε = −0.4‰) was smaller than −1.8‰ using eq 6 which was consistent with the carbon isotope change below 1.5‰ of TCE aqueous diffusion in low permeability sediments estimated by Wanner and Hunkeler.[6] We note, however, that such residual concentrations would come to lie below the sensitivity of current compound-specific isotope analysis. On the basis of the results from this and other studies,[6,13,45] we therefore recommend that conservative interpretations of CSIA field data may be accomplished if an additional uncertainty in carbon isotope values of ±1‰ is considered in addition to the present analytical uncertainty of ±2‰ suggested by EPA.[49] This would apply to contaminations by chlorinated solvents and gasoline contaminants (but not natural gases such as methane or ethane) and would be adequate to consider the effect of aqueous diffusion and dispersion (but not the influence from sorption, volatilization or gas phase diffusion). Compared to recent predictions from simulations[15,19,37,38,41] this significantly reduces uncertainties and enables more reliable interpretation of CSIA data in the field (e.g., source identification or discrimination, assessment of degradation).

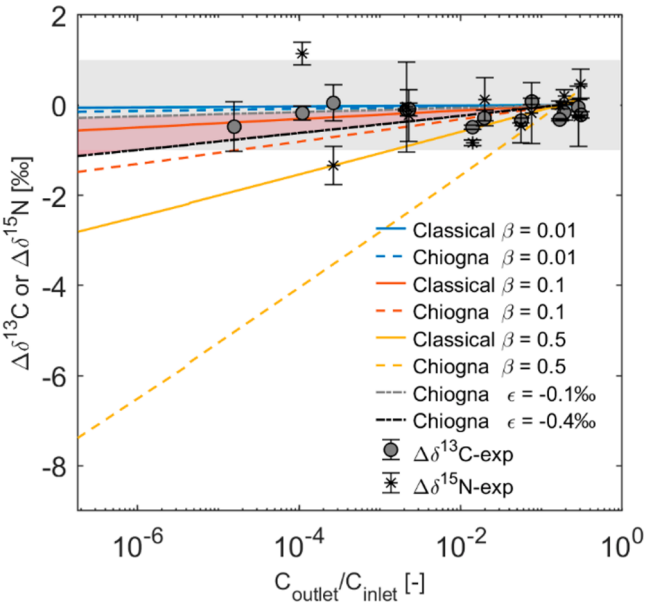

Figure 6. Simulated isotope fractionations $\Delta\delta^{13}C$ or $\Delta\delta^{15}N$ induced by transverse dispersion at different outlet-to-inlet concentration ratios C_{outlet}/C_{inlet} using different β-values and ε-values. Solid lines: with classical linear parametrization of transverse dispersion; dashed lines: with nonlinear parametrization by Chiogna et al.; we used light and heavy isotopologues of BAM (M_L= 190.02 Da, M_H = 191.02 Da) as the target compounds, with $D_L = 6.08 \times 10^{-10}$ m²/s. Both dispersion scenarios with the transverse dispersion coefficient $D_t = 2.99 \times 10^{-9}$ m²/s fitted to the experimental concentration data, with the effective grain size d_{eff} = 1.0 mm in the classical equation, and d_{eff} = 2.5 mm in eq 6 from Chiogna et al. Gray zone represents the ±1‰ tolerated standard deviation of the original standard isotope value. Red zone represents the isotope fractionation range predicted using eq 6 from Chiogna et al. with ε = −0.1 (gray dotted-dashed line) and −0.4‰ (black dotted-dashed line).

■ ASSOCIATED CONTENT

Supporting Information

The Supporting Information is available free of charge at https://pubs.acs.org/doi/10.1021/acs.est.0c06741.

https://doi.org/10.1021/acs.est.0c06741
Environ. Sci. Technol. 2021, 55, 4772−4782

More detailed experimental section and description of the numerical simulations (PDF)

AUTHOR INFORMATION

Corresponding Author

Martin Elsner − *Institute of Groundwater Ecology, Helmholtz Zentrum München, 85764 Neuherberg, Germany; Chair of Analytical Chemistry and Water Chemistry, Technical University of Munich, 81377 Munich, Germany;* orcid.org/0000-0003-4746-9052; Phone: +49 89 2180-78232; Email: m.elsner@tum.de

Authors

Fengchao Sun − *Institute of Groundwater Ecology, Helmholtz Zentrum München, 85764 Neuherberg, Germany; Chair of Analytical Chemistry and Water Chemistry, Technical University of Munich, 81377 Munich, Germany*

Jan Peters − *Institute of Groundwater Ecology, Helmholtz Zentrum München, 85764 Neuherberg, Germany; Center for Applied Geoscience, University of Tübingen, 72074 Tübingen, Germany*

Martin Thullner − *Department of Environmental Microbiology, UFZ—Helmholtz Centre for Environmental Research, 04318 Leipzig, Germany;* orcid.org/0000-0001-9723-4601

Olaf A. Cirpka − *Center for Applied Geoscience, University of Tübingen, 72074 Tübingen, Germany*

Complete contact information is available at: https://pubs.acs.org/10.1021/acs.est.0c06741

Author Contributions

The manuscript was written through the contributions of all authors. All authors have given approval to the final version of the manuscript.

Funding

This work was funded by an ERC consolidator grant ("'MicroDegrade"', grant no. 616861) awarded by the European Research Council.

Notes

The authors declare no competing financial interest.

ACKNOWLEDGMENTS

We acknowledge Armin H. Meyer from Helmholtz Zentrum München for his contribution on the isotope measurements of the toluene samples from the tank experiment.

REFERENCES

(1) Elsner, M. Stable isotope fractionation to investigate natural transformation mechanisms of organic contaminants: Principles, prospects and limitations. *J. Environ. Monit.* **2010**, *12* (11), 2005−31.

(2) Kuntze, K.; Eisenmann, H.; Richnow, H.-H.; Fischer, A. Compound-specific stable isotope analysis (CSIA) for evaluating degradation of organic pollutants: An overview of field case studies. In *Anaerobic Utilization of Hydrocarbons, Oils, and Lipids*; Boll, M., Ed. Springer: Cham: 2019; pp 323−360.

(3) Elsner, M.; Imfeld, G. Compound-specific isotope analysis (CSIA) of micropollutants in the environment - Current developments and future challenges. *Curr. Opin. Biotechnol.* **2016**, *41*, 60−72.

(4) Elsner, M.; Jochmann, M. A.; Hofstetter, T. B.; Hunkeler, D.; Bernstein, A.; Schmidt, T. C.; Schimmelmann, A. Current challenges in compound-specific stable isotope analysis of environmental organic contaminants. *Anal. Bioanal. Chem.* **2012**, *403* (9), 2471−91.

(5) Thullner, M.; Centler, F.; Richnow, H.-H.; Fischer, A. Quantification of organic pollutant degradation in contaminated aquifers using compound specific stable isotope analysis − Review of recent developments. *Org. Geochem.* **2012**, *42* (12), 1440−1460.

(6) Wanner, P.; Hunkeler, D. Carbon and chlorine isotopologue fractionation of chlorinated hydrocarbons during diffusion in water and low permeability sediments. *Geochim. Cosmochim. Acta* **2015**, *157*, 198−212.

(7) Jin, B.; Rolle, M.; Li, T.; Haderlein, S. B. Diffusive fractionation of BTEX and chlorinated ethenes in aqueous solution: Quantification of spatial isotope gradients. *Environ. Sci. Technol.* **2014**, *48* (11), 6141−50.

(8) Kopinke, F. D.; Georgi, A.; Voskamp, M.; Richnow, H. H. Carbon isotope fractionation of organic contaminants due to retardation on humic substances: Implications for natural attenuation studies in aquifers. *Environ. Sci. Technol.* **2005**, *39*, 6052.

(9) Elsner, M.; McKelvie, J.; Lacrampe Couloume, G.; Sherwood Lollar, B. Insight into methyl tert-butyl ether (MTBE) stable isotope fractionation from abiotic reference experiments. *Environ. Sci. Technol.* **2007**, *41* (16), 5693−5700.

(10) Hofstetter, T. B.; Schwarzenbach, R. P.; Bernasconi, S. M. Assessing transformation processes of organic compounds using stable isotope fractionation. *Environ. Sci. Technol.* **2008**, *42* (21), 7737−7743.

(11) Schmidt, T. C.; Schirmer, M.; Weiss, H.; Haderlein, S. B. Microbial degradation of methyl tert-butyl ether and tert-butyl alcohol in the subsurface. *J. Contam. Hydrol.* **2004**, *70*, 173.

(12) Kuder, T.; Wilson, J. T.; Kaiser, P.; Kolhatkar, R.; Philp, P.; Allen, J. Enrichment of stable carbon and hydrogen isotopes during anaerobic biodegradation of MTBE: Microcosm and field evidence. *Environ. Sci. Technol.* **2005**, *39*, 213.

(13) Wanner, P.; Hunkeler, D. Isotope fractionation due to aqueous phase diffusion - What do diffusion models and experiments tell? - A review. *Chemosphere* **2019**, *219*, 1032−1043.

(14) LaBolle, E. M.; Fogg, G. E.; Eweis, J. B.; Gravner, J.; Leaist, D. G. Isotopic fractionation by diffusion in groundwater. *Water Resour. Res.* **2008**, *44* (7), W07405.

(15) Rolle, M.; Jin, B. Normal and inverse diffusive isotope fractionation of deuterated toluene and benzene in aqueous systems. *Environ. Sci. Technol. Lett.* **2017**, *4* (7), 298−304.

(16) O'Leary, M. H. Measurement of the isotope fractionation associated with diffusion of carbon dioxide in aqueous solution. *J. Phys. Chem.* **1984**, *88* (4), 823−825.

(17) Zhang, T.; Krooss, B. M. Experimental investigation on the carbon isotope fractionation of methane during gas migration by diffusion through sedimentary rocks at elevated temperature and pressure. *Geochim. Cosmochim. Acta* **2001**, *65* (16), 2723−2742.

(18) Schloemer, S.; Krooss, B. M. Molecular transport of methane, ethane and nitrogen and the influence of diffusion on the chemical and isotopic composition of natural gas accumulations. *Geofluids* **2004**, *4* (1), 81−108.

(19) Rolle, M.; Chiogna, G.; Bauer, R.; Griebler, C.; Grathwohl, P. Isotopic fractionation by transverse dispersion: Flow-through microcosms and reactive transport modeling study. *Environ. Sci. Technol.* **2010**, *44* (16), 6167−6173.

(20) Kopinke, F. D.; Georgi, A.; Roland, U. Isotope fractionation in phase-transfer processes under thermodynamic and kinetic control - Implications for diffusive fractionation in aqueous solution. *Sci. Total Environ.* **2018**, *610−611*, 495−502.

(21) Kopinke, F.-D.; Georgi, A. H/D-isotope fractionation due to aqueous phase diffusion − Deuterated hydrocarbons revisited. *Chemosphere* **2020**, *258*, 127357.

(22) Jähne, B.; Heinz, G.; Dietrich, W. Measurement of the diffusion coefficients of sparingly soluble gases in water. *J. Geophys. Res.* **1987**, *92* (C10), 10767−10776.

(23) Einstein, A. *Investigations on the Theory of the Brownian Movement*; Courier Corporation: North Chelmsford, MA, 1956.

(24) Maxwell, J. C. On the dynamical theory of gases. *Proc. R. Soc. London* **1866**, *15*, 167−171.

(25) Lemons, D. S.; Gythiel, A. Paul Langevin's 1908 paper "On the theory of Brownian motion" ["Sur la théorie du mouvement brownien," C. R. Acad. Sci. (Paris) 146, 530−533 (1908)]. *Am. J. Phys.* **1997**, *65* (11), 1079−1081.
(26) Ali, S. M.; Samanta, A.; Ghosh, S. K. Mode coupling theory of self and cross diffusivity in a binary fluid mixture: Application to Lennard-Jones systems. *J. Chem. Phys.* **2001**, *114* (23), 10419−10429.
(27) Tyrrell, H. J. V.; Harris, K. *Diffusion in Liquids: A Theoretical and Experimental Study*; Butterworth-Heinemann: Waltham, MA, 2013.
(28) Wanner, P.; Hunkeler, D. Molecular dynamic simulations of carbon and chlorine isotopologue fractionation of chlorohydrocarbons during diffusion in liquid water. *Environ. Sci. Technol. Lett.* **2019**, *6* (11), 681−685.
(29) Tyroller, L.; Brennwald, M. S.; Busemann, H.; Maden, C.; Baur, H.; Kipfer, R. Negligible fractionation of Kr and Xe isotopes by molecular diffusion in water. *Earth Planet. Sci. Lett.* **2018**, *492*, 73−78.
(30) Tyroller, L.; Brennwald, M. S.; Mächler, L.; Livingstone, D. M.; Kipfer, R. Fractionation of Ne and Ar isotopes by molecular diffusion in water. *Geochim. Cosmochim. Acta* **2014**, *136*, 60−66.
(31) Bourg, I. C.; Richter, F. M.; Christensen, J. N.; Sposito, G. Isotopic mass dependence of metal cation diffusion coefficients in liquid water. *Geochim. Cosmochim. Acta* **2010**, *74* (8), 2249−2256.
(32) Rodushkin, I.; Stenberg, A.; Andrén, H.; Malinovsky, D.; Baxter, D. C. Isotopic fractionation during diffusion of transition metal ions in solution. *Anal. Chem.* **2004**, *76* (7), 2148−2151.
(33) Bhattacharyya, S.; Bagchi, B. Power law mass dependence of diffusion: A mode coupling theory analysis. *Phys. Rev. E: Stat. Phys., Plasmas, Fluids, Relat. Interdiscip. Top.* **2000**, *61* (4), 3850.
(34) Scheidegger, A. E. General theory of dispersion in porous media. *J. Geophys. Res.* **1961**, *66* (10), 3273−3278.
(35) De Josselin de Jong, G. Longitudinal and transverse diffusion in granular deposits. *Trans., Am. Geophys. Union* **1958**, *39* (1), 67−74.
(36) Chiogna, G.; Eberhardt, C.; Grathwohl, P.; Cirpka, O. A.; Rolle, M. Evidence of compound-dependent hydrodynamic and mechanical transverse dispersion by multitracer laboratory experiments. *Environ. Sci. Technol.* **2010**, *44* (2), 688−693.
(37) Xu, S.; Sherwood Lollar, B.; Sleep, B. E. Rethinking aqueous phase diffusion related isotope fractionation: Contrasting theoretical effects with observations at the field scale. *Sci. Total Environ.* **2017**, *607−608*, 1085−1095.
(38) Eckert, D.; Rolle, M.; Cirpka, O. A. Numerical simulation of isotope fractionation in steady-state bioreactive transport controlled by transverse mixing. *J. Contam. Hydrol.* **2012**, *140−141*, 95−106.
(39) Eckert, D.; Qiu, S.; Elsner, M.; Cirpka, O. A. Model complexity needed for quantitative analysis of high resolution isotope and concentration data from a toluene-pulse experiment. *Environ. Sci. Technol.* **2013**, *47* (13), 6900−7.
(40) Worch, E. Eine neue gleichung zur berechnung von diffusionskoeffizienten gelöster stoffe. *Vom Wasser* **1993**, *81*, 289−297.
(41) Van Breukelen, B. M.; Rolle, M. Transverse hydrodynamic dispersion effects on isotope signals in groundwater chlorinated solvents' plumes. *Environ. Sci. Technol.* **2012**, *46* (14), 7700−8.
(42) Stokes, R. H. An improved diaphragm-cell for diffusion studies, and some tests of the method. *J. Am. Chem. Soc.* **1950**, *72* (2), 763−767.
(43) Asfour, A. F. A. Improved and simplified diaphragm cell design and analysis technique for calibration. *Rev. Sci. Instrum.* **1983**, *54* (10), 1394−1396.
(44) Bauer, R. D.; Maloszewski, P.; Zhang, Y.; Meckenstock, R. U.; Griebler, C. Mixing-controlled biodegradation in a toluene plume–Results from two-dimensional laboratory experiments. *J. Contam. Hydrol.* **2008**, *96* (1−4), 150−68.
(45) Wanner, P.; Parker, B. L.; Chapman, S. W.; Aravena, R.; Hunkeler, D. Does sorption influence isotope ratios of chlorinated hydrocarbons under field conditions? *Appl. Geochem.* **2017**, *84*, 348−359.
(46) Tempest, K. E.; Emerson, S. Kinetic isotopic fractionation of argon and neon during air−water gas transfer. *Mar. Chem.* **2013**, *153*, 39−47.
(47) Seltzer, A. M.; Ng, J.; Severinghaus, J. P. Precise determination of Ar, Kr and Xe isotopic fractionation due to diffusion and dissolution in fresh water. *Earth Planet. Sci. Lett.* **2019**, *514*, 156−165.
(48) Schurner, H. K.; Maier, M. P.; Eckert, D.; Brejcha, R.; Neumann, C. C.; Stumpp, C.; Cirpka, O. A.; Elsner, M. Compound-specific stable isotope fractionation of pesticides and pharmaceuticals in a mesoscale aquifer model. *Environ. Sci. Technol.* **2016**, *50* (11), 5729−39.
(49) Hunkeler, D.; Meckenstock, R. U.; Sherwood Lollar, B.; Schmidt, T. C.; Wilson, J.; Schmidt, T.; Wilson, J. *A Guide for Assessing Biodegradation and Source Identification of Organic Ground Water Contaminants Using Compound Specific Isotope Analysis (CSIA)*; US EPA: Oklahoma, 2008; https://purl.fdlp.gov/GPO/LPS115694.

https://doi.org/10.1021/acs.est.0c06741
Environ. Sci. Technol. 2021, 55, 4772−4782